Universal properties of interacting Brownian motors

Yashar Aghababaie,* Gautam I. Menon, and Michael Plischke
Department of Physics, Simon Fraser University, Burnaby, British Columbia, Canada V5A 1S6
(Received 19 August 1998)

We study the effects of interactions in ratchet models for one-dimensional Brownian motors. In these models, directed motion of a single particle (the motor) is produced by subjecting it to the action of a one-dimensional time-dependent asymmetric potential and thermal noise. We consider here the collective behavior of a finite density of such motors that move on a line and interact with each other through excluded volume interactions. We show that the density-density correlation function, calculated in the steady state, exhibits dynamical scaling at long wavelengths and times. Our Monte Carlo simulations support the conjecture that the hydrodynamic properties of interacting Brownian motors are governed by the Kardar-Parisi-Zhang universality class [Phys. Rev. Lett. **56**, 889 (1986)]. We demonstrate numerically that the effective noise governing the stochastic dynamics in a coarse-grained version of our model has short-range spatial correlations. Our results should be applicable to a wide variety of models for Brownian motors with short-range interactions. [S1063-651X(99)01802-4]

PACS number(s): 05.40.Jc, 87.10.+e, 05.60.Cd, 87.19.Rr

I. INTRODUCTION

Molecular motors are proteins or protein complexes that transduce chemical energy into mechanical work. Ignoring molecular detail, these motors (kinesins, dyneins, and myosins) can be visualized as compact objects moving with a net drift velocity along a line (a tubulin filament for kinesins and dyneins, an actin filament for myosins). Such motors play an important role in the transport of cargo along the axons of nerve cells, muscle contraction, and cell motility [1,2].

While the three families of molecular motors differ in detail, they share a few common physical properties. First, there is a directionality to the motion of such molecules that, for linear motors, can be associated with the polarity of the tracks on which they move. Second, the tracks themselves can be idealized as rigid, periodic, one-dimensional structures [3]. Third, the irreversible conversion of the chemical energy obtained from adenosine triphosphate hydrolysis into work breaks detailed balance. Finally, all molecular motors operate in a regime dominated by the randomizing effects of Brownian noise. Such noise has zero mean and hence cannot, acting alone, produce directed motion. Molecular motors must therefore ''rectify'' Brownian forces if they are to exhibit a drift velocity in the absence of a net time-averaged force. The problem of modeling molecular motors can thus be set in the more general context of ''Brownian motor'' or ''thermal ratchet'' models for the extraction of useful work from thermal fluctuations.

Models for Brownian motors can be divided into the following three classes [3–8]: *A*, ''fluctuating force'' models, in which a point particle is placed in a periodic, asymmetric time-independent potential and subjected to a stochastic force with non-Gaussian correlations; *B*, ''fluctuating potential'' models, in which the particle is driven both by Gaussian white noise and a time-dependent asymmetric potential; and *C*, ''particle fluctuating between states'' models, in which the particle is driven by Gaussian white noise, while an internal state of the particle determines the static asymmetric potential it experiences. This internal state is itself determined by a stochastic dynamics that does not obey detailed balance. The combination of a single particle with an asymmetric (ratchet) potential, thermal noise, and an external forcing that violates detailed balance is called a thermal ratchet.

The models we study here generalize models of type *B* to incorporate a finite density of interacting particles. We address the following question: What is the appropriate hydrodynamic description of density fluctuations in a collection of interacting Brownian motors on a ring? We will assume these interactions to be of a simple excluded volume form, although any interparticle interaction that is neither too long ranged nor allows particles to interpenetrate should yield the same results. At the level of nonuniversal properties, earlier work has shown that excluded volume interactions can affect both the magnitude and the direction of the current in a nontrivial manner [9]. In contrast, we study here the scaling behavior of fluctuations in the nonequilibrium steady state of such an interacting system to extract universal features of models for interacting Brownian motors. Universality implies that our conclusions should be independent of the detailed nature of the potential chosen, the density of interacting particles, and the switching rate between potential states, except possibly at isolated points in parameter space. Most aspects of the discussion here should apply to fluctuating force (class *A*) and particle fluctuating between states (class *C*) models as well, provided the time correlations of the fluctuating force or the stochastic interstate dynamics are not too long ranged.

For simplicity, we study latticized versions of our (in general) continuum models and examine the scaling properties of the intermediate scattering function $S_\rho(k,t)$ defined by

$$S_\rho(k,t)=\frac{1}{N}\langle \delta\rho(k,0)\,\delta\rho(-k,t)\rangle, \tag{1.1}$$

*Present address: Department of Physics, McGill University, 3600 University Street, Montreal, Quebec, Canada H3A 2T8.

where N is the number of particles, k is $2n\pi/L$, $n=0,\pm1,\pm2,\ldots,L/2$, and L is the system size. Here $\delta\rho(k,t)$ is the Fourier component with wave vector k of the deviation from the mean local density, $\delta\rho(x,t)=\rho(x,t)-\langle\rho(x)\rangle$, with the angular brackets denoting a time average.

Transforming the density field $\rho(x,t)$ to a ''height'' field $h(x,t)$ via $\rho(x,t)=\partial_x h(x,t)$ and imposing helical boundary conditions on $h(x,t)$ to satisfy the constraint $\int_0^L\rho(x,t)=h(L)-h(0)=N$, $S_\rho(k,t)$ can be related to the structure factor

$$S(k,t)=\langle\delta h(k,0)\,\delta h(-k,t)\rangle, \tag{1.2}$$

where $\delta h(k,t)$ is the Fourier transform of $h(x,t)-\langle h(x)\rangle$. For small k and large t, i.e., in the hydrodynamic limit, if $S(k,t)$ exhibits dynamical scaling, we can write

$$S(k,t)\sim k^{-2+\eta}F(k^z t), \tag{1.3}$$

where η and z are scaling exponents and F is a scaling function.

The basic result of this paper is that these scaling properties are described by the Kardar-Parisi-Zhang (KPZ) [10] equation. This Langevin equation [10]

$$\frac{\partial h}{\partial t}=\nu\nabla^2 h+\frac{\lambda}{2}(\nabla h)^2+\zeta(\mathbf{x},t) \tag{1.4}$$

describes the long-time, long-wavelength behavior of a number of nonequilibrium systems [11,12]. Equation (1.4) is written in a form appropriate for surface models, where $h(\mathbf{x},t)$ is the height, relative to a d-dimensional substrate, of a growing interface and $\zeta(\mathbf{x},t)$ represents Gaussian white noise. This equation was originally proposed as a generalization of the Edwards-Wilkinson (EW) equation [13] ($\lambda=0$ in the above) to describe the interfacial width of clusters in the Eden model as well as the scaling properties of several other models for interface growth. The KPZ and EW equations govern distinct universality classes of dynamical behavior with scaling solutions characterized by the exponents z and η. The exponent η determines the long-wavelength properties of equal-time height-height correlations in the steady state (the conventional roughness exponent α is related to η through $\eta=1-2\alpha$), while z describes the wave-vector dependence of relaxation functions. For the KPZ equation, owing to the existence of a fluctuation-dissipation theorem, these exponents can be obtained exactly for $d=1$ and take on the values $z=3/2$ and $\eta=0$. The exact solution of the linear EW equation yields $z=2$ and $\eta=0$.

An intuitive way of understanding the relation of models for interacting Brownian motors to the KPZ equation is the following. Coarse-grain microscopic configurations of such models in space and time. At spatial scales larger than the repeat distance ℓ of the periodic potential and on time scales much larger than the typical time scale τ over which the potential changes, the system will appear to have a constant density on average, as well as a constant current. Superimposed on this constant density are spontaneous fluctuations that obey a local conservation law. The effects of interparticle interactions at the largest length scales can be summarized in the following observation: These density fluctuations are convected with a speed that depends on their magnitude.

Consider now an apparently unrelated model, that of the stochastic dynamics of a finite density ρ of hard-core particles on a line, which hop individually with rate $(1+\epsilon)/2$ to the right and $(1-\epsilon)/2$ to the left, provided the excluded volume constraint is satisfied. Such a system, the ''asymmetric exclusion process'' (ASEP) for $\epsilon\neq0$, has a net particle current $J=\epsilon\rho(1-\rho)$. The symmetry breaking that results in a constant current in the ASEP is an explicit consequence of the asymmetry in the hopping rates. This symmetry breaking is to be contrasted with the more subtle symmetry breaking in the case of the ratchet models, where a net current is obtained by switching between rates that individually satisfy detailed balance.

Density-density correlations for the ASEP are known to be governed by KPZ exponents [14] through a Bethe ansatz solution of the associated quantum model in the fully asymmetric ($\epsilon=1$) limit [15,16] and extensive numerical work in the more general partially asymmetric case. Since both models share the feature expected to be most relevant to a hydrodynamic description, the existence of a nontrivial density-dependent current, it is reasonable to conjecture that they should belong to the same universality class, irrespective of the fact that the detailed origin of the symmetry breaking is different in each case.

The organization of this paper is as follows. In Sec. II we describe the two models we study in this work. Section III discusses the relevant theory. We prove that the current as a function of density is symmetric about half filling for a large class of interacting ratchet models, including ours. We review briefly previous work on driven diffusive systems and provide a (nonrigorous) derivation of a continuum equation for the time evolution of the particle density. In Sec. IV we describe the Monte Carlo simulations we have performed to test dynamical universality in interacting Brownian motors. We present conclusions and possible directions for further study in Sec. V.

II. MODELS

In the simplest versions of the fluctuating potential models [5,6,8] individual motor particles experience a time-dependent potential $V(x,t)=\eta(t)U(x)$ in addition to random Brownian forces with zero mean value. Here $U(x)$ is periodic with period ℓ, i.e., $U(x+\ell)=U(x)$, and an asymmetric function of x, i.e., $U(x)\neq U(-x)$. The time dependence of $V(x,t)$ is governed by a (stochastic or deterministic) switching function $\eta(t)$, which takes the values 0 and 1. For concreteness and in agreement with previous work on noninteracting Brownian motors, we will assume $U(x)$ to be of the sawtooth form

$$\begin{aligned} U(x)&=ax \quad (0\leq x\leq\alpha\ell)\\ &=b(\ell-x) \quad (\alpha\ell\leq x\leq\ell),\end{aligned} \tag{2.1}$$

with $a,b>0$, $a\alpha\ell=b\ell(1-\alpha)$, and $\alpha<1$. The switching of the potential occurs independently of the state of the motors, thus breaking detailed balance. Together with the lack of reflection symmetry in $U(x)$, this switching generates a net particle current. Therefore, Brownian motors exhibit macroscopic motion along a periodic potential by extracting useful work from nonequilibrium fluctuations.

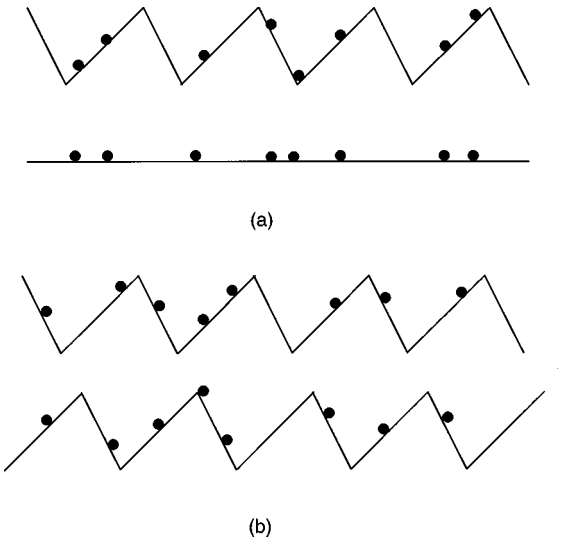

FIG. 1. Schematic representation of models. The filled circles represent particles. In (a), depicting model I, hard-core particles can sit on either a pinning potential (here a skew sawtooth) or a flat potential. In (b) model II is shown. The particles can sit on one of two sawtooth potentials, which are shifted relative to each other by half the potential period. In both cases the switching between potentials is configuration independent, while the rates for the particles' movement on each of the potentials satisfies detailed balance.

We can see how this current arises with the following argument. In the ''flat'' state of the potential for which $\eta=0$ [see Fig. 1(a)], a single particle will diffuse isotropically. When the potential is switched to the ''up'' or $\eta=1$ state, it is more likely to be found in a region of space where it experiences a net force to the left than to the right. Repeated cycling between $\eta=0$ and $\eta=1$ states generates a net motion of the particle.

Our first model, which we will call model I, generalizes the above model for the action of a single Brownian motor to a finite number N of interacting motors on a one-dimensional lattice. These motors hop to unoccupied nearest neighbor sites with rates determined by the discretized potential in Eq. (2.1). Our discretization ensures that a motor occupies only one lattice site at a time and the hard-core constraint implies that at most one motor occupies a single lattice site.

Our second model, model II, differs from model I in the choice of the two potential states experienced by the motors. Each particle now experiences a potential $V(x,t)=\eta(t)U(x)+[1-\eta(t)]U(x+\ell/2)$. The flat potential in model I is thus replaced with a shifted version of the periodic potential. In this case the current is a result of the particles sliding to the valley of the sawtooth. When the potential is switched, particles in energetically unfavorable locations slide to the valleys of the new potential. In both models repetition of the switching procedure results in a net time-averaged current.

We use periodic boundary conditions in the numerical simulations described here. In both models an elementary step consists of either an attempt of a particle to hop to a neighboring site or an attempt to switch the potential. The transition rates between configurations satisfy detailed balance with Metropolis rates, $P(\{\overline{\sigma'}\}\rightarrow\{\overline{\sigma}\})=\min(1,\exp[H(\{\overline{\sigma'}\})-H(\{\overline{\sigma}\})])$. Here $\{\sigma\}$ indexes allowed configurations of the motors on the lattice and $H(\{\sigma\})$ is the energy of the configuration. The switching of the potentials occurs stochastically and is governed by an exponential distribution of waiting times.

The parameters in the models are the following. Each period of the potential contains W lattice sites, all of which we assign to the segment of the potential with positive slope. The length of the system L is measured in periods of the sawtooth. The maximum height of the sawtooth potential is V and we define $r=\exp[-V/k_BT(W-1)]$. Finally, the parameters P_{01} and P_{10} represent the probabilities that the potential changes from $\eta=0$ to $\eta=1$ and vice versa.

In terms of these parameters the hopping probabilities on the sawtooth are chosen to be

$$P(i\rightarrow i+1)=\begin{cases}\dfrac{r}{1+r} & \text{if } 0\leqslant i<W-1\\ \dfrac{1}{1+r^{W-1}} & \text{if } i=W-1,\end{cases}$$

$$P(i+1\rightarrow i)=\begin{cases}\dfrac{1}{1+r} & \text{if } 0\leqslant i<W-1\\ \dfrac{r^{W-1}}{1+r^{W-1}} & \text{if } i=W-1,\end{cases}$$

where we have indexed the lattice sites from 0 at the potential minimum.

III. THEORY

A number of driven lattice gases with excluded volume interactions exhibit a current density $J(\rho)$ that is symmetric about $\rho=\frac{1}{2}$. Two examples are the ASEP (or the biased random walk), where $J(\rho)$ is parabolic about $\rho=1/2$, and models with strong disorder [17], where the current is a more complicated function of density.

This exact particle-hole symmetry is a feature of the models we study as well and can be obtained through simple arguments. Consider a finite density ρ of particles moving in the time-dependent ratchet potential $V(x,t)$ defined in the preceding section. The time-averaged particle current can only be a function of the time-dependent potential $V(x,t)$ and the density ρ. The statement of particle-hole symmetry is then

$$J(\rho;V(x,t))=J(1-\rho;V(x,t)), \tag{3.1}$$

which relates currents at densities ρ and $1-\rho$ for the *same* microscopic time-dependent potential.

Note now that the relation

$$J(\rho;V(x,t))=-J(1-\rho;-V(x,t)) \tag{3.2}$$

holds exactly. To see this, consider the one-to-one mapping between particle configurations at density ρ and ''hole'' or ''vacancy'' configurations at density $1-\rho$, where holes are assigned to sites that are unoccupied in the particle configuration. Every particle hop, say to the right, corresponds uniquely to the hopping of a hole in the opposite direction (left) at the same rate. The hole current thus precisely equals

the negative of the particle current. The hopping rates for the holes can be obtained from the hopping rates for the particles by reversing particle hopping rates about each bond. It is easy to see that such rates can be derived from the potential $-V(x,t)$ for the Metropolis rates used in this paper and more generally for any update scheme that uses rates that satisfy detailed balance.

To prove Eq. (3.1) it is thus sufficient to show

$$J(\rho;V(x,t))=-J(\rho;-V(x,t)). \tag{3.3}$$

A strategy that works for the potentials we consider here is to consider the parity transformed potential $V^R(x,t)$, obtained from the definition $V^R(x,t)=V(-x,t)$. Such a parity transformation is equivalent to interchanging the definitions of left and right and cannot alter the magnitude of the current. We thus have

$$J(\rho,V^R(x,t))=-J(\rho,V(x,t)). \tag{3.4}$$

Since $V(x,t)$ is not reflection symmetric, this relation between currents for different ratchet potentials related to each other by a parity transformation is a nontrivial one.

For sawtooth potentials of the type defined in Eq. (2.1), $V^R(x,t)$ and $-V(x,t)$ are related through a trivial shift [of $a\alpha\ell$ in the y direction and $\ell(1-\alpha)$ in the x direction]. This shift cannot change the net current as it merely corresponds to a choice of the zero of the potential (which is irrelevant to the calculation of forces and hence hopping rates) and of the origin. Putting these results together we now have

$$J(\rho,-V(x,t))=J(\rho,V^R(x,t))=-J(\rho,V(x,t)), \tag{3.5}$$

thus proving Eq. (3.1).

While our proof is exact for sawtooth potentials of the type discussed here [and more generally for periodic potentials whose Fourier coefficients (a_n,b_n) are related through $\tan(n\theta)=a_n/b_n$ with θ a non-trivial angle], we believe that particle-hole symmetry may hold more generally in similar lattice gas models for interacting Brownian motors. Indeed, for the disordered fully asymmetric exclusion process, such particle-hole symmetry holds to a high degree of numerical accuracy [17]. This feature is not well understood, although there have been recent attempts at a proof of this result [18]. We note in passing that there do exist excluded volume models of motors that do not display particle-hole symmetry [9]. These models, however, are not lattice gas models but continuum ones where the numerical discretization is not scaled to the particle size.

We now describe a phenomenological derivation of the KPZ equation from simple hydrodynamic arguments [12]. Consider our microscopic model for interacting Brownian motors and coarse grain the density field of the interacting motors over the microscopic period ℓ of the potential. The density field is now uniform on average, with a time-averaged value of ρ_0. Coarse graining in time over time scales larger than the period τ over which the potential changes eliminates the microscopic time scale associated with the switching of the potential. At length and time scales much larger than ℓ and τ, we are dealing with a system that is, on average, uniform in both space and time.

The exact conservation of particle number must hold for the coarse-grained density field and can be expressed in the form of a continuity equation

$$\frac{\partial\rho(x,t)}{\partial t}=-\partial_x J(\rho(x,t),\partial_x\rho(x,t),\ldots), \tag{3.6}$$

where $J(\rho(x,t),\partial_x\rho(x,t),\ldots)$ is the particle current. This current is, in general, a function of $\rho(x,t)$ as well as its gradients. Decomposing the density field as

$$\rho(x,t)=\rho_0+\delta\rho(x,t),\quad \int_0^L dx\ \delta\rho(x,t)=0, \tag{3.7}$$

we can expand

$$\begin{aligned} &J(\rho(x,t),\partial_x\rho(x,t),\ldots)\\ &\quad=J(\rho_0)-c_0\delta\rho(x,t)-\frac{1}{2}c_1(\delta\rho)^2\\ &\qquad-D\partial_x\delta\rho-\zeta(x,t)+\cdots. \end{aligned} \tag{3.8}$$

Here c_0 is the ''kinematic wave velocity'' or the group velocity with which density fluctuations in the system are convected, c_1 is the coefficient of the relevant nonlinear term, D is a diffusion coefficient, and $\zeta(x,t)$ represents the effects of random fluctuations. Restoring these terms to the equation of motion and ignoring higher-order irrelevant terms, we obtain an equation derived by van Beijeren, Kutner, and Spohn in the context of one-dimensional driven lattice gases [14]:

$$\begin{aligned} \frac{\partial\delta\rho(x,t)}{\partial t}&=c_0\partial_x\delta\rho(x,t)+c_1\delta\rho(x,t)\partial_x\delta\rho(x,t)\\ &\quad+D\partial_x^2\delta\rho(x,t)+\partial_x\zeta(x,t). \end{aligned} \tag{3.9}$$

This equation without the noise term [i.e., $\zeta(x,t)=0$] was originally studied by Burgers in the context of the one-dimensional Navier-Stokes equation. The correspondence between the KPZ equation and the noisy Burgers equation can be seen as follows. We first perform a Galilean transformation on the Burgers equation to remove the linear term in $\partial_x\delta\rho$; this is equivalent to transforming to the comoving frame of the density wave. Using $\delta\rho(x,t)=\partial_x h(x,t)$ and substituting in Eq. (3.9), we obtain the KPZ equation [Eq. (1.4)].

To map particle configurations in our lattice model to height configurations, associate a surface element with slope 1 to a particle and a slope of -1 to a vacancy or hole. The dynamics of the height field is related to the dynamics of the particles in the following way: A particle hop to the left from site i is identified with an evaporation event from site i, while a particle hop to the right corresponds to deposition or growth at site $i+1$ [19–21]. A net current in the particle language then translates into a surface that grows on average at a constant rate. This mapping between particle configurations and height configurations follows the ''single-step'' model defined in Ref. [20], although the underlying particle dynamics that generates the dynamics of the height field is more complicated in our case.

Critical exponents are typically measured through correlation functions. In our simulations we measured the relaxation function [14]

$$\Phi(k,t) \equiv \frac{\langle \hat{\rho}(-k,0)\hat{\rho}(k,t)\rangle - \langle \hat{\rho}(-k,0)\rangle\langle \hat{\rho}(k,t)\rangle}{\langle \hat{\rho}(-k,0)\hat{\rho}(k,0)\rangle - \langle \hat{\rho}(-k,0)\rangle\langle \hat{\rho}(k,0)\rangle} = \frac{S_\rho(k,t)}{S_\rho(k,0)} \tag{3.10}$$

in the comoving frame of reference. Although Φ is properly a function of the two variables k and t separately, the dynamical scaling hypothesis suggests that it can be written in the form $\Phi(k^z t)$ for an appropriately chosen z. As shown initially by Forster, Nelson, and Stephen [22] for the randomly forced Burgers equation and later by Kardar, Parisi, and Zhang [10] for surface growth, z is $\frac{3}{2}$ in one dimension. The free-field or Edwards-Wilkinson value is $z=2$ [13].

In addition, we measured the value of the hydrodynamic exponent η through the steady-state structure factor

$$S(k) = \lim_{t\to\infty} \langle \hat{h}_k(t)\hat{h}_{-k}(t)\rangle, \tag{3.11}$$

where

$$\hat{h}_k(t) = \frac{1}{(LW)^{1/2}} \sum_{j=1}^{LW} [h_j(t) - \langle h_j(t)\rangle]\, e^{ijk}.$$

The structure factor diverges for small k as $k^{-2+\eta}$, where $\eta=0$ for both the EW and KPZ equations.

IV. COMPUTER SIMULATIONS

In this section we outline the Monte Carlo (MC) algorithm used in our simulations and present our numerical results. In our simulations, we measured time in units of MC steps (MCS), where a single MC step consists of N cycles of the basic algorithmic step. In each cycle we attempted either a switching of the potential or a particle move. Our most extensive studies were done with parameter values that maximized the current, i.e., at half filling for the models considered here. This choice minimizes the crossover from the EW regime to KPZ behavior since λ is proportional to the curvature of the J vs ρ curve, which is maximized at half filling.

We used $W=10$ lattice sites per well in all of our simulations. For model I we took $r=0.05$, $P_{01}=0.03$, and $P_{10}=0.04$. For model II the parameter values used were $r=0.01$ and $P_{01}=P_{10}=0.02$. Typically we waited $(2\times10^4)-(5\times10^4)$ MCS for the system to equilibrate before recording data for currents and correlation functions. The quantities $\Phi(k,t)$ and $S(k,t)$ were averaged over 10^4 configurations for $L\leqslant128$, while we averaged over 3×10^3 configurations for $L=256$.

The $J(\rho)$ vs ρ curves for models I and II are shown in Figs. 2 and 3. The symmetry of the curves about $\rho=1/2$ is very accurate for large L, in accord with the theoretical expectation of particle-hole symmetry.

We measured the critical exponents of our models z and η through the relaxation function $\Phi(k,t)$ and the structure factor $S(k)$, respectively. In order to discount small wavelength correlations of the density due to the potential shape, we coarse grained the density over one potential period by summing the occupations of the interior sites and assigning this number to a single (reduced) site. The largest lattice we considered in detail had $L=256$ wells; the discretization to 10 sites per well implies that our systems had at most 2560 lattice sites.

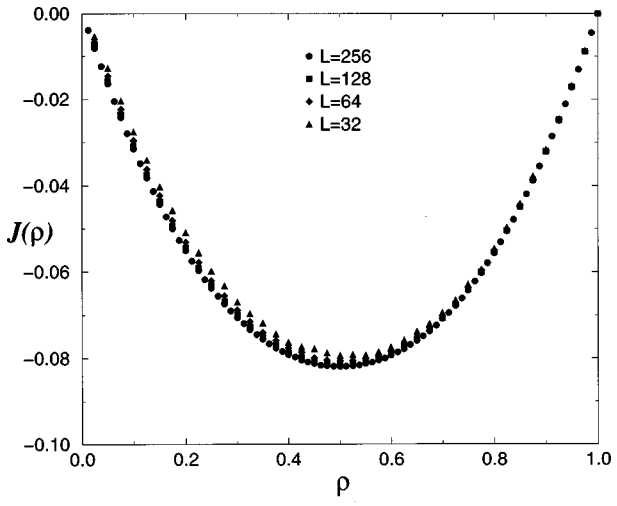

FIG. 2. Dependence of the steady-state current $J(\rho)$ on the average density ρ of particles for model I with $32\leqslant L\leqslant256$.

An estimate of the effective dynamical exponent $z_{eff}(L,\rho)$ was obtained in the following way. The data for $\Phi(k,t)$ for a given density and system size were plotted as functions of the scaled variables $k^z t$ for various z. The value of z that provided the best visual collapse of the data was taken to be z_{eff}. Examples of this data collapse are shown in Figs. 4 and 5 for models I and II at half filling for $L=128$, yielding $z_{eff}=1.60$ and 1.59, respectively. For both models, the relaxation function generically has two distinct branches. For the smallest value of k, $k=2\pi/L$, the relaxation function decays more slowly than for larger values of k. Both figures contain data for $k=2\pi j/L$ for $j\leqslant5$. For $j>1$ the data collapse to high accuracy onto a single curve. This separation of

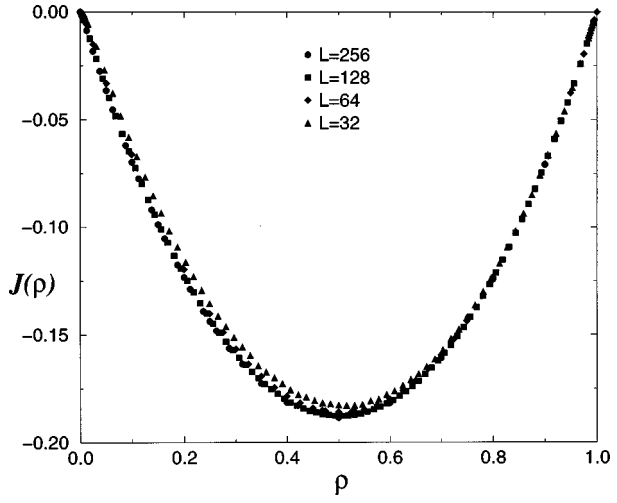

FIG. 3. Dependence of the steady-state current $J(\rho)$ on the average density ρ for model II with $32\leqslant L\leqslant256$.

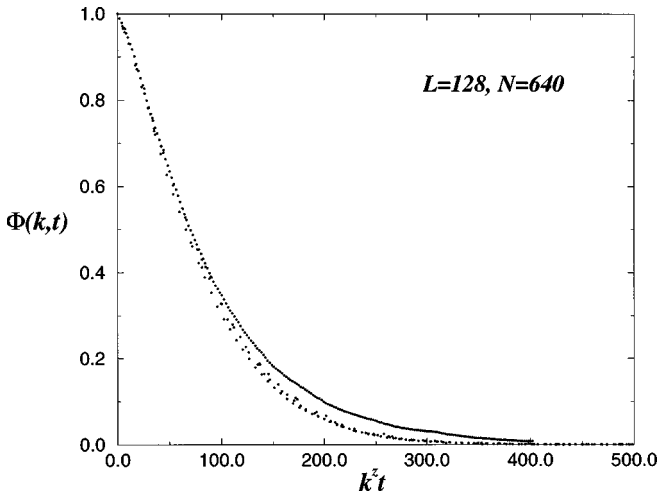

FIG. 4. Relaxation function $\Phi(k,t)$ for model I for $L=128$ and $\rho=0.5$ plotted as a function of the scaled variable $k^z t$ for $z=1.60$. We show data for the five smallest values of $k=2\pi j/L$, with $j=1, 2, 3, 4,$ and 5.

the relaxation function into two branches (with $j=1$ the special case) is also a feature of the single-step model [20].

We have carried out this analysis systematically for $L=32-256$ as a function of ρ. The effective exponents $z_{eff}(L,\rho)$ for models I and II are plotted as functions of ρ in Figs. 6 and 7, respectively. The conservative error bars reflect the somewhat subjective procedure of identifying the ''best'' value of z by inspection. However, the systematic dependence of this effective exponent on both ρ and L is quite striking. First, it is clear that the data support the conclusion $z_{eff}(L,\rho)=z_{eff}(L,1-\rho)$, consistent with the general particle-hole symmetry discussed above for the current. Second, there is a systematic decrease of the effective exponent z_{eff} as L is increased for all $\rho\neq 0$, with the smallest values occurring at $\rho=0.5$, as expected theoretically. The smallest value of z was found to be 1.58 ± 0.01 for model I and 1.56 ± 0.01 for model II, calculated in both cases for $L=256$. We conclude that in the thermodynamic limit $z(\rho)$ approaches

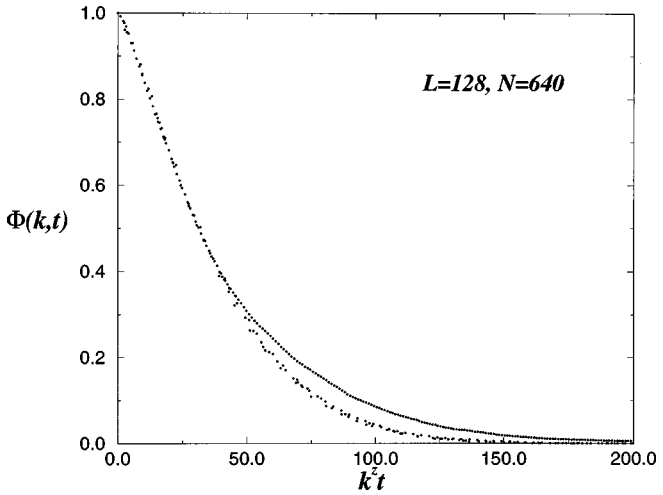

FIG. 5. Relaxation function $\Phi(k,t)$ for model II for $L=128$ and $\rho=0.5$ plotted as a function of $k^z t$ for $z=1.59$. The values of k are the same as in Fig. 4.

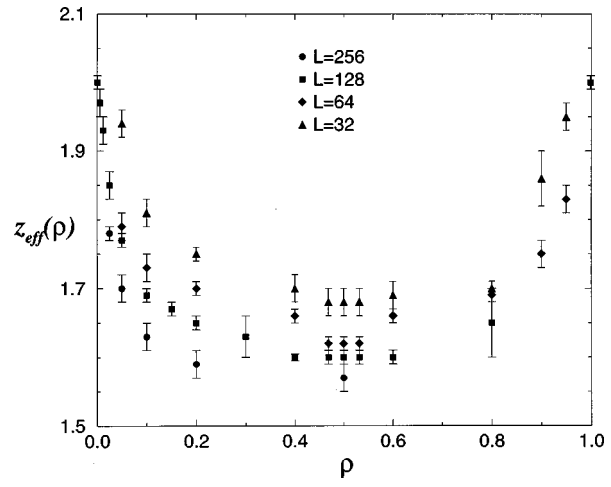

FIG. 6. Effective exponent $z_{eff}(L,\rho)$ plotted as a function of ρ for model I and systems of size $32\leqslant L\leqslant 256$. Note the systematic decrease of z_{eff} as L is increased at constant density.

the value $\frac{3}{2}$, consistent with the predictions of the KPZ equation.

We have also calculated the hydrodynamical exponent η through the time-independent structure factor in Eq. (3.11). For both models we found $\eta=0.0\pm 0.01$ for all densities and all system sizes.

If one assumes that the KPZ equation describes these models then one can in fact predict the dependence of the measured effective exponent z_{eff} on L, following recent work by Neergaard and den Nijs [23] on crossover scaling functions appropriate to one-dimensional growth models in the KPZ universality class. Neergaard and den Nijs provide the asymptotic form

$$m\simeq A/L^{z_0}+B/L^{z_1}. \tag{4.1}$$

Here A and B are constant for fixed KPZ coupling constant λ, m is the mass gap of the associated finite (of size L) spin chain, and z_0 and z_1 are the dynamical critical exponents associated with the EW and KPZ universality classes, i.e., $z_0=2$ and $z_1=1.5$. The effective exponent $z_{eff}(L)$ is ob-

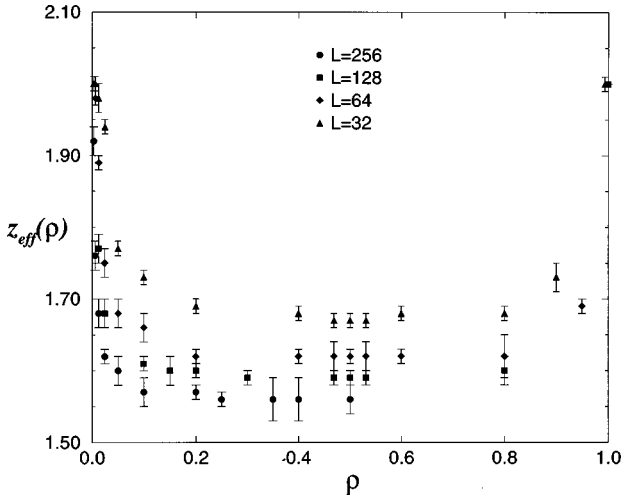

FIG. 7. Effective exponent $z_{eff}(L,\rho)$ for model II.

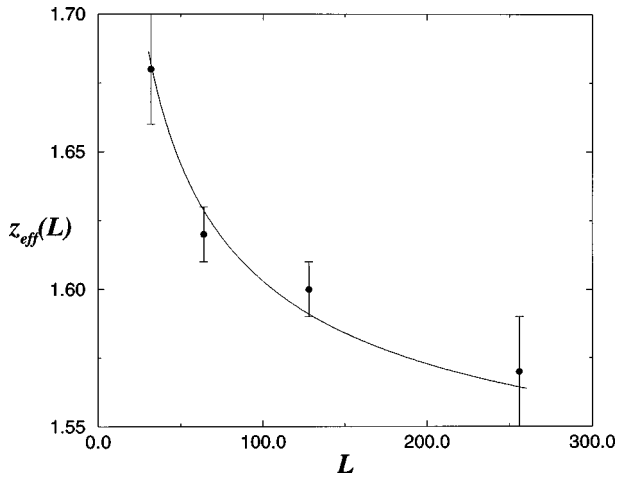

FIG. 8. Effective exponent $z_{eff}(L,\rho)$ plotted as a function of L for $\rho=0.5$ for model I. The curve is a fit to the functional form (4.2) obtained from the KPZ equation.

tained from $z_{eff}(L)=-\partial(\ln m)/\partial(\ln L)$. If z_{eff} is close to 1.5, simple algebra gives the leading L dependence as

$$z_{eff}(L)\simeq 1.5+C/\sqrt{L}, \tag{4.2}$$

where C is a constant. This indicates that the approach to the asymptotic value of 1.5 is of a square root form. Figures 8 and 9 show that an approximate fit to such a correction is consistent with the data, although there are large inherent errors in this procedure given that the measured z_{eff} is obtained directly from a simulation.

We have implicitly assumed that the effective noise governing the behavior of interacting Brownian motors is short ranged in both space and time. This is an important issue since correlated noise is known to affect the scaling properties of the KPZ equation [24]. We have studied the validity of this assumption through an approximate numerical procedure related to the ''inverse method'' introduced by Lam and Sander [25] to study the effective hydrodynamic equation governing the behavior of interface models in the KPZ and EW universality class. To illustrate this procedure, assume

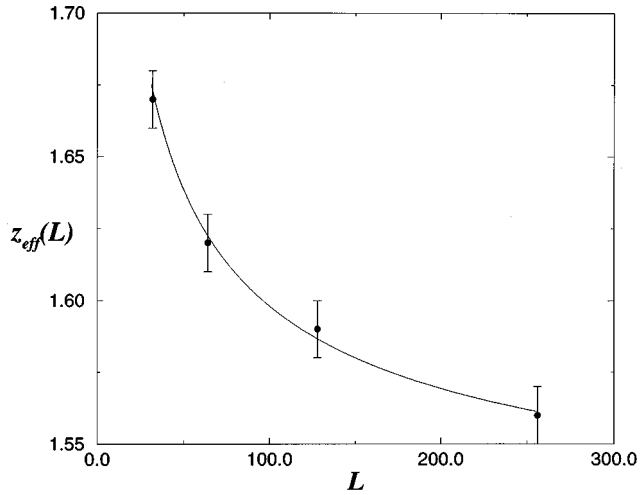

FIG. 9. Effective exponent $z_{eff}(L,\rho)$ plotted as a function of L for $\rho=0.5$ for model II. As in Fig. 6, the curve is a fit to Eq. (4.2).

that the effective equation governing the dynamics of the height variable $h(x,t)$ in our models can be written as

$$\frac{\partial h}{\partial t}=F(\partial_x h,\partial_x^2 h,\ldots)+\eta(x,t)\,. \tag{4.3}$$

We have grouped the terms governing the deterministic evolution of the surface into $F(\partial_x h,\partial_x^2 h,\ldots)$, in general allowing for more complex (although irrelevant in the hydrodynamic limit) terms than those retained in the KPZ equation. We have also separated the noise terms into $\eta(x,t)$, which we assume, without loss of generality, to have zero mean value.

Evolving the surface configuration at time t forward to $h(x,t+\Delta t)$, we can write the effective noise term as

$$\left(\frac{h(x,t+\Delta t)-h(x,t)-F(\partial_x h,\partial_x^2,\ldots)\Delta t}{\Delta t}\right)=\eta(x,t)\,. \tag{4.4}$$

Note that this procedure generates an ensemble of values for the stochastic noise term $\eta(x,t)$. We can now compute the equal-time correlations of the noise by averaging $\langle\eta(x,t)\,\eta(x',t)\rangle$ obtained from Eq. (4.4), by evolving systems initially chosen to be representative of the steady state [26].

To implement this procedure, we generated a sequence of k typical steady-state configurations $(C_1,C_2,\ldots,C_k)$ for model I by evolving the system for 2×10^4 MCS. Each of these configurations in turn was evolved for a short time Δt using m different initial random seeds. Such a procedure generates inequivalent histories of the system starting from the same steady-state configuration. The deterministic part of the evolution for the ith typical initial profile can then be extracted from

$$F_i(\partial_x h,\partial^2 h,\ldots)\Delta t=\frac{1}{m}\sum_{j=1}^{m}\left[h_j^i(x,t+\Delta t)-h_j^i(x,t)\right]. \tag{4.5}$$

Once this has been obtained, the equal-time noise-noise correlation function can be constructed for each of the C_k configurations by averaging over stochastic histories. We also average over the ensemble of initial steady-state configurations. Our results are displayed for model I with $L=32$ in Fig. 10. It is clear that any spatial correlations are extremely short ranged and clearly not of the power-law form required to affect the exponents z and η [24,27].

V. CONCLUSIONS

In this paper we have presented numerical evidence and intuitive arguments to support the conjecture that the hydrodynamic properties of interacting Brownian motors belong to the universality class of the Kardar-Parisi-Zhang equation. This conjecture was motivated by the reasonable guess that microscopic configurations in such models, upon appropriate coarse graining, should yield the same macroscopic physics as the ASEP.

We now discuss models of types A and C defined in the Introduction. In view of the generality of the results we de-

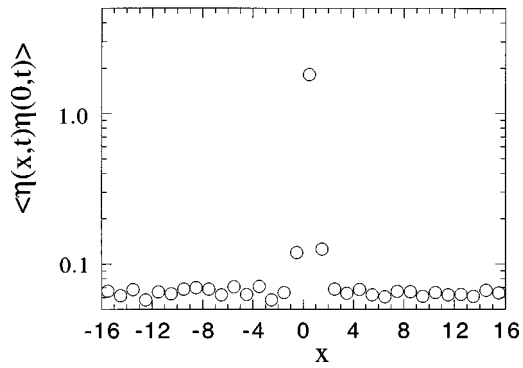

FIG. 10. Equal-time noise correlator $\langle \eta(x,t)\,\eta(0,t)\rangle$ for model I with $L=32$ and $\rho=0.5$.

scribe here, which depend only on the fact that expanding the uniform particle current in the density field to second order yields a relevant KPZ nonlinearity, we would expect that the hydrodynamic properties of these models should be governed by KPZ exponents, as is the case here. The only caveats are the following. In general, while KPZ scaling would be expected in the asymptotic limit, the approach to this limit may be obscured by crossover effects. These are model specific and, in general, some optimization might be required for such asymptotic scaling to be easily visible. Also, the coefficient of the nonlinear term λ may vanish at isolated points in parameter space for general models. In such cases, one would expect EW exponents precisely at those points and crossover behavior in their vicinity. Finally and perhaps most importantly, the effective noise governing the microscopic degrees of freedom must have only finite-range correlations in space and time. For the KPZ equation with colored noise, a smooth variation of dynamical exponents such as z has been predicted if the noise has sufficiently long-range correlations [24]. It is not obvious that the hydrodynamic properties of interacting Brownian motors with an effective colored noise can be mapped directly onto an appropriately generalized KPZ equation. However, we reiterate that the results of Sec. IV indicate that the effective noise is spatially uncorrelated at least for the models we study here.

The effects of microscopic disorder has been discussed for single Brownian motors. Such disorder can be modeled in terms of a disruption of the perfect periodicity of the ratchet potential [28]. For the models we consider here, it is natural to conjecture that the hydrodynamic behavior is governed by the same equation that governs the ASEP with quenched disordered hopping rates. Incorporating the most relevant terms due to such disorder leads to the following variant of the KPZ equation:

$$\frac{\partial h}{\partial t}=c(x)\partial_x h+\nu\partial_x^2 h+\frac{\lambda}{2}(\partial_x h)^2+\zeta(\mathbf{x},t), \qquad (5.1)$$

with $c(x)=c_0+c_1(x)$, where $c_1(x)$ is a random variable with short-range spatial correlations [17]. Interestingly, it has been argued that the vanishing of the average kinematic wave velocity (c_0 above) renders the pure KPZ fixed point unstable. As a consequence, the hydrodynamic properties of interacting ratchets with disorder might be expected to be governed by a fixed point other than the KPZ or EW fixed points at special points or in special regions of parameter space. We are currently studying this problem.

Finally, the ASEP with open boundary conditions and with particle injection and removal at the two boundaries at different rates has been studied extensively in recent years, using different matrix methods [29]. The nonequilibrium phase diagram of such systems contains distinct phases with different macroscopic properties. Such boundary conditions are natural for the biological problem and it is interesting to speculate that control in such systems might be exerted by changing the rates at which motors are allowed to hop onto and leave the filament at either end. An investigation of these problems is currently under way [30].

ACKNOWLEDGMENTS

We have benefited from conversations with R. Mukhopadhyay, F. Jülicher, J. Prost, and M. Siegert. This research was supported by the NSERC of Canada.

[1] F. Jülicher, A. Ajdari, and J. Prost, Rev. Mod. Phys. **69**, 1269 (1997).
[2] R. D. Astumian, Science **276**, 917 (1997).
[3] R. D. Astumian and M. Bier, Phys. Rev. Lett. **72**, 1766 (1994).
[4] M. Magnasco, Phys. Rev. Lett. **71**, 1477 (1993); see also I. Derényi, C. Lee, and A.-L. Barabási, *ibid.* **80**, 1473 (1998) for an application of this model to nonequilibrium growth processes.
[5] J. Prost, J. Chauwin, L. Peliti, and A. Ajdari, Phys. Rev. Lett. **72**, 2652 (1994).
[6] F. Jülicher and J. Prost, Phys. Rev. Lett. **75**, 2618 (1995).
[7] C. R. Doering, W. Horsthemke, and J. Riordan, Phys. Rev. Lett. **72**, 2984 (1994).
[8] L. Schimansky-Geier, M. Kschischo, and T. Fricke, Phys. Rev. Lett. **79**, 3335 (1997).
[9] I. Derényi and T. Vicsek, Phys. Rev. Lett. **75**, 374 (1995); I. Derényi and A. Ajdari, Phys. Rev. E **54**, R5 (1996).
[10] M. Kardar, G. Parisi, and Y. C. Zhang, Phys. Rev. Lett. **56**, 889 (1986).
[11] See A.-L. Barabási and H. E. Stanley, *Fractal Concepts in Surface Growth* (Cambridge University Press, Cambridge, 1995) for a review of much of this work, especially in the context of nonequilibrium surface growth.
[12] J. Krug and H. Spohn, in *Solids Far from Equilibrium: Growth, Morphology and Defects*, edited by C. Godrèche (Cambridge University Press, Cambridge, 1991).
[13] S. F. Edwards and D. R. Wilkinson, Proc. R. Soc. London, Ser. A **381**, 17 (1982).
[14] H. van Beijeren, R. Kutner, and H. Spohn, Phys. Rev. Lett. **54**, 2026 (1985).
[15] D. Dhar, Phase Transit. **9**, 51 (1987).
[16] L.-H. Gwa and H. Spohn, Phys. Rev. A **46**, 844 (1992).
[17] G. Tripathy and M. Barma, Phys. Rev. Lett. **78**, 3039 (1997); e-print cond-mat/9711302.

[18] K. M. Kolwanker and A. Punnoose, e-print cond-mat/9807246.
[19] Z. Rácz, *Phase Transitions, Critical Fluctuations, and Scaling in Nonequilibrium Steady States* (University of Geneva, Geneva, 1996).
[20] M. Plischke, Z. Rácz, and D. Liu, Phys. Rev. B **35**, 3485 (1987).
[21] See, for example, *Dynamics of Fractal Surfaces*, edited by F. Family and T. Vicsek (World Scientific, Singapore, 1991).
[22] D. Forster, D. R. Nelson, and M. J. Stephen, Phys. Rev. A **16**, 732 (1977).
[23] J. Neergaard and M. den Nijs, Phys. Rev. Lett. **74**, 730 (1995).
[24] E. Medina, T. Hwa, M. Kardar, and Y. C. Zhang, Phys. Rev. A **39**, 3053 (1989).
[25] C.-H. Lam and L. M. Sander, Phys. Rev. Lett. **71**, 561 (1993).
[26] Unequal time correlations can also be calculated in principle by autocorrelating $\langle \eta(x,t)\,\eta(x,t')\rangle$ obtained from Eq. (4.4). However, a numerical implementation of this procedure is problematic since $F(\partial_x h, \partial_x^2 h, \ldots)$ is not known exactly.
[27] We have checked explicitly that our results are independent of the time discretization required in Eq. (4.4).
[28] T. Harms and R. Lipowsky, Phys. Rev. Lett. **79**, 2895 (1997).
[29] J. Krug, Phys. Rev. Lett. **67**, 1882 (1991); B. Derrida, E. Domany, and D. Mukamel, J. Stat. Phys. **69**, 667 (1992).
[30] G. I. Menon and M. Siegert (unpublished).